Archives of Acoustics Vol. 49, No. 3, pp. 439–445 (2024), doi: 10.24425/aoa.2024.148800

Research Paper

Influence of Ultrasonic Cavitation on *Botryococcus Braunii* Growth

Asleena SALAEH

Division of Physics, School of Science, Walailak University
Thailand; e-mail: as.salaeh@gmail.com

(*received November 9, 2023; accepted April 3, 2024; published online June 25, 2024*)

This study investigates ultrasonic energy's impact on enhancing the growth of *Botryococcus braunii* (*B. braunii*) microalgae. Microalgae, known for their advantages in greenhouse gas mitigation and biomass conversion, were subjected to various stressors, including ultrasonic waves, to optimize productivity. Ultrasonic waves induce acoustic cavitation, increasing membrane permeability and substrate conversion. The study examined the impact of energy and maximum pressure resulting from bubble collapse on the relative specific growth rate of *B. braunii* microalgae. It was observed that reproduction showed a promotive trend until the energy surpassed 30 kJ. However, when ultrasonic energy reached 18.2 kJ, reproduction was inhibited due to the maximum pressure generated during bubble bursting, which reached 5.7 $\mu N/\mu m^2$, leading to the suppression of reproduction upon encountering bubble collapse events. Under specific ultrasonic conditions (15.1 kJ energy, maximum pressure of 45.5×10^5 Pa), a maximum specific growth rate of 0.329 ± 0.020 day^{-1} in a two-day interval boosted *B. braunii* microalgae biomass productivity. These findings advance our understanding of ultrasonic wave effects on microalgae reproduction and underscore the potential for optimizing ultrasonic parameters to enhance biomass production.

Keywords: *Botryococcus braunii*; ultrasonic wave; cavitation; specific growth rate; bubble size.

Copyright © 2024 The Author(s).
This work is licensed under the Creative Commons Attribution 4.0 International CC BY 4.0 (https://creativecommons.org/licenses/by/4.0/).

1. Introduction

Microalgae offer numerous benefits over conventional crops, such as rapid growth, ease of cultivation, and space efficiency (Enmak, 2010). Notably, microalgae can mitigate the greenhouse effect by converting carbon dioxide into biomass via photosynthesis, thereby lowering greenhouse gas levels in the atmosphere, and supporting carbon sequestration (Onyeaka *et al.*, 2021).

Despite the challenges of microalgae cultivation, their unique characteristics make them attractive for industrial applications. To fully exploit their potential, researchers have explored various environmental stressors, including nutrient scarcity, high temperatures, intense light, and elevated pH levels (Shakirov *et al.*, 2021; Fu *et al.*, 2019). Innovative technologies such as ultrasonic waves have been used to apply controlled stress conditions, promoting cell proliferation and optimizing metabolic activity.

Ultrasonic waves, generated through cavitation, employ low-energy waves to stimulate cells. The implosion of cavities near the cell surface enhances membrane permeability, facilitating nutrient and molecule exchange. Research confirms that low-energy ultrasonic waves significantly increase *Botryococcus braunii* (*B. braunii*) growth rates compared to conditions without them (Wang *et al.*, 2014; Xu *et al.*, 2014). This study primarily aims to develop ultrasonic wave stimulation for enhanced *B. braunii* growth and biomass production.

2. Theory of acoustic cavitation

The Rayleigh–Plesset equation is a second-order ordinary differential equation that governs the dynamics of a spherical bubble within an infinite fluid. It plays a crucial role in understanding cavitation phenomena and predicting the behavior of such a bubble. The Rayleigh–Plesset equation is expressed as follows:

$$\rho_0 \left[R\ddot{R} + \frac{3}{2}\dot{R}^2 \right] = (p_v - p_\infty(t)) + p_{g0}\left(\frac{R_0}{R}\right)^{3k} - \frac{2S}{R} - 4\mu\frac{\dot{R}}{R}, \tag{1}$$

where $\dot{R}$ and $\ddot{R}$ are the first- and second-order derivatives of the bubble radius with respect to time, R_0 is the initial bubble radius in meters [m], ρ_0 is the density of fluid in kilograms per cubic meter [kg/m^3], S is the surface tension in Newtons per meter [N/m], μ is the dynamic viscosity of fluid in Pascal-second [Pa·s], p_v is the vapor pressure of fluid, p_{g0} is the gas pressure in the bubble at its ambient state ($p_{g0} = p_0 + \frac{2S}{R_0} - p_v$), and $p_\infty(t)$ is the variation in bulk pressure as function of time, which is given by Eq. (2):

$$p_\infty(t) = p_0 - p_A \sin(2\pi f t), \tag{2}$$

where p_0 is the ambient pressure (1 atm, 101.325 kPa), f is the frequency [Hz], p_A is the driving pressure [Pa] that is correlated with the acoustic intensity (I_{ac}) and acoustic power (Wang, Yuan, 2016):

$$p_A = \sqrt{2 I_{\mathrm{ac}} \rho_0 c_0}, \tag{3}$$

$$I_{\mathrm{ac}} = \frac{\text{Power}}{\text{Volume or area}}, \tag{4}$$

where c_0 is the speed of sound in fluid in meters per second [m/s]. Ultrasonic waves impact microalgae cells through cavitation, a phenomenon that occurs when ultrasonic waves pass through a substance. These waves create alternating regions of compression and rarefaction as they propagate. During the rarefaction phase, vapor bubbles can form within the liquid medium, leading to cavitation. As the ultrasonic wave continues to exert pressure on the medium, these bubbles grow until they reach a critical size. When this happens, the bubbles collapse rapidly during the compression phase.

When the cavitation bubble grows to a significant size, the effects of non-condensable gas, surface tension, and viscosity become negligible. As a result, the complex Rayleigh–Plesset equation in Eq. (1) can be simplified to:

$$\rho_0 \left[R\ddot{R} + \frac{3}{2}\dot{R}^2 \right] = \left(p_v - p_\infty(t)\right). \tag{5}$$

During the collapse phase, when the applied pressure exceeds the vapor pressure ($p_\infty > p_v$) and the bubble radius decreases ($R < R_0$), the interface velocity can be described as follows:

$$\dot{R} \cong -\sqrt{\frac{2(p_\infty - p_v)}{3\rho_0}\left(\left(\frac{R_0}{R}\right)^2 - 1\right)}. \tag{6}$$

The force generated by the collapse of cavitation bubbles plays a significant role in both promoting and disrupting microalgae cells. This force is influenced by the initial size of the cavitation bubbles, which, in turn, depends on the frequency of the ultrasonic waves. This relationship can be expressed through Eq. (7) (Brennen, 2005):

$$f_n = \frac{1}{2\pi}\sqrt{\frac{1}{\rho_0 R_e^2}\left(3k\left(p_0 - p_v\right) + \frac{2S}{R_e}\left(3k - 1\right)\right)}, \tag{7}$$

where k is approximately constant, S is the surface tension, R_e is the equilibrium radius at pressure (p_0), and ($p_0 - p_v$) represents tension of the fluid.

When a bubble collapses near a cell wall or cell membrane, it can cause disruption or alteration in the shape of a microalgae cell (Liu *et al.*, 2022). This effect occurs when the bubble experiences a stress exceeding its yield strength, resulting in actual deformation. To comprehend how a collapsing bubble can generate such high pressure, the maximum pressure ($p_{\max}$) in Pascals [Pa] can be approximated using Eq. (8):

$$p_{\max} \cong 0.157(p_\infty - p_v)\left(\frac{R_0}{R}\right)^3 + p_\infty. \tag{8}$$

Furthermore, this maximum pressure occurs at a distance ($r_{\max}$) in meters [m] from the bubble center, given by Eq. (9):

$$r_{\max} \cong 1.59\, R. \tag{9}$$

3. Material and methods

3.1. Microalgae and culture conditions

Plankton samples were collected from the reservoir at Walailak University in Nakhon Si Thammarat, Thailand (latitude 8°38′32.25″N, longitude 99°54′26.52″E) using a plankton net with a mesh size of 67 µm. This reservoir stores brackish water with a slow flow, a pH of 7.2, and a dissolved oxygen level of 6.47 mg/L (Rubsai, 2012). Colonies of *B. braunii* were isolated from the collected samples and cultured individually in 5 ml of BG-11 liquid medium for one month. They were then transferred to 250 ml flasks with 100 ml of BG-11 medium for a week. Subsequently, 10 ml of *B. braunii* algae were divided and cultivated in separate 1000 ml flasks with 800 ml of BG-11 medium, resulting in 13 distinct experimental conditions. The cultures were maintained in a sterile chamber at a constant temperature of 25 °C, with 3000 lux illumination during a 16:8-hour light-dark period. The structure of *B. braunii* microalgae is illustrated in Fig. 1. In *B. braunii* microalgae, ovoid cells form tetrad patterns at the colony center. As colonies develop, these cells enlarge and transform into conical

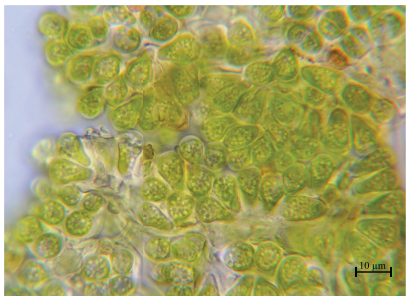

Fig. 1. *Botryococcus braunii* microalgae.

cells, playing a crucial role in defining the outer boundaries (Gupte, 2012).

3.2. Ultrasonic treatment and experiments

The investigation utilized an ultrasonic bath (Elmasonic P60H), operating at frequencies of 37 kHz and 80 kHz, with a 5.75-liter tank. Microalgae were subjected to ultrasonic excitation at specific power levels: 57.2 W, 83.6 W, and 132.3 W for 37 kHz, and 46.3 W, 67.2 W, and 101.2 W for 80 kHz (refer to Table 1). Exposure durations were precisely 3 min and 5 min, with 2-day intervals. Optimal excitation parameters were determined based on the study by Salaeh *et al.* (2017). Each stimulation with ultrasonic wave for all condition was conducted at 9.00 a.m. Thailand time according to these specified conditions. After ultrasonic treatment, microalgae samples were cultured under consistent flask conditions. Each experimental condition was replicated three times to ensure reliability. Biomass measurements were recorded every third day throughout the study.

The effective ultrasonic power of the system was assessed by measuring the power of the ultrasonic bath at different temperatures. This measurement was essential as the application of power to the system induces energy transfer to the liquid, resulting in molecular movement and the generation of thermal energy. The power of the ultrasonic bath (P, in W) can be calculated using Eq. (10) (Liu *et al.*, 2022):

$$P = mC_p \frac{\Delta T}{\Delta t}, \tag{10}$$

where m is the mass of fluid, C_p is the specific heat capacity of fluid, ΔT is the temperature difference between the initial temperature and the final temperature after a specific reaction time Δt.

3.3. Microalgae growth and biomass measurement

A 1 ml sample of *B. braunii* cells was transferred to a tube for counting cell density using a hemocytometer slide. The sample was carefully placed on the slide, covered, and observed under an optical microscope (Olympus CH20i microscope). Daily counting of the microalgae with a microscope allowed for precise determination of the specific growth rate of *B. braunii* microalgae. Cell density calculations were conducted by capturing images of microalgae samples within a hemocytometer under a microscope. The cell count was determined through image processing, followed by calculating the cell density using Eq. (11) (Dilia *et al.*, 2018):

$$\text{Cell density} = \frac{\text{Number of counted cells} \times 25 \times 10^4}{\text{Number of boxs}}. \tag{11}$$

The growth data from cultivating *B. braunii* under different ultrasonic parameters validated the presented logistic model. The logistic model of population growth is written as follows (Zhang *et al.*, 2016):

$$N(t) = \frac{KN_0}{N_0 + (K - N_0)\, e^{-rt}}, \tag{12}$$

where N is the number of cells as a function of time t, K is the maximum number of cells or the carrying capacity, and r is the specific growth rate.

Biomass content was determined by measuring the dry weight-to-volume ratio (mg/ml). A 12 ml algae aliquot was centrifuged, filtered onto a weighed 47 mm glass fiber filter, dried at 103 °C for 13 hours, and then weighed. Biomass productivity (g (L day)$^{-1}$) is defined as follows (Chen *et al.*, 2016):

$$\text{Biomass productivity} = \frac{B_2 - B_1}{t_2 - t_1}, \tag{13}$$

where B_1 and B_2 represent the biomass concentration at times t_1 and t_2, respectively, representing the initial and final points.

4. Results and discussion

4.1. The behaviors of acoustic cavitation within ultrasonic bath

Acoustic cavitation occurs due to pressure fluctuations induced by ultrasonic waves in a fluid. These waves compress and rarefy the fluid, forming cavitation bubbles that explosively collapse, enlarging until reaching resonance velocity. This implosion generates pores near cell membranes, enhancing permeability. Ultrasonic treatment holds potential for improved substrate conversion through enhanced diffusion (Ren *et al.*, 2019; Pereira *et al.*, 2023). Multiple factors in Table 1, including the maximum cavitation radius ($R_{\max}$), maximum pressure ($p_{\max}$) during collapse, and

Table 1. Numerical results of cavitation bubble dynamics.

Frequency [kHz]	Power [W]	Intensity [mW/cm^2]	R_0 [μm]	$R_{\max}$ [μm]	$R_{\min}$ [μm]	$\frac{R_{\max}}{R_{\min}}$	$\dot{R}$	$p_{\max}$ ($\times 10^5$ Pa)	$r_{\max}$ [μm]
37	57.2	4.9	74	141.5	41.7	3.4	49.77	5.0	66.4
	83.6	7.2		145.5	21.7	6.71	140.2	45.5	34.5
	132.3	11.4		150.4	14.5	10.41	271.5	173.1	23.0
80	46.3	4.0	35	61.4	16.9	3.63	55.2	6.3	26.9
	67.2	5.8		63.5	14.7	4.3	72.29	11.5	23.3
	101.2	8.7		65.9	9.1	7.2	156.49	56.9	14.5

the distance ($r_{\max}$) from the bubble center where the maximum pressure occurs, are influenced by ultrasonic parameters and liquid characteristics.

The numerical results on the dynamic behavior of cavitation bubbles for stimulated microalgae in an ultrasonic bath are summarized in Table 1, presenting the following characteristics. According to the experiment, the medium's density (ρ_m) is 1001.68 kg/m^3, and its sound speed (c_m) is 1353.22 m/s, which is nearly equal to that of water. Consequently, the dynamic viscosity and applied surface tension were 0.00891 Pa·s and 0.0072 N/m, respectively. The relationship between ultrasonic power and intensity is described by Eq. (4), wherein increasing ultrasonic power enhances the stretching effect of the ultrasonic wave on cavitation formation in the positive pressure region (Hao *et al.*, 2021).

The maximum size of the cavitation bubble was calculated by solving Eq. (1) using the numerical method. During the expansion phase, the bubble grows until it reaches its maximum size ($R_{\max}$) before collapsing. Importantly, the $R_{\max}$ is inversely related to the emitted ultrasonic frequency. According to Eq. (7), the initial bubble size is 74 μm and 35 μm at ultrasonic frequencies of 37 kHz and 80 kHz, respectively. The ratio of maximum bubble size to initial bubble size increases with higher ultrasonic power. Specifically, at 37 kHz, the ratio ranges from 1.91 to 2.03, while at 80 kHz, it ranges from 1.75 to 1.88. It is important to note that the ratio of bubble size at 80 kHz is relatively lower due to reduced acoustic pressure in the ultrasonic bath and the smaller wavelength (λ) compared to the 37 kHz ultrasonic frequency. During the collapse phase (from $R_{\max}$ to $R_{\min}$), the $p_{\max}$ increases with ultrasonic power for each frequency. For instance, at 37 kHz, with power levels of 57.2 W, 83.6 W, and 132.3 W, $R_{\max}$ is 141.5 μm, 145.5 μm, and 150.4 μm, respectively. The maximum pressure points are situated at distances of 66.4 μm, 34.5 μm, and 23.0 μm away from the bubble as it collapses. Similarly, at an ultrasonic frequency of 80 kHz, with power levels of 46.3 W, 67.2 W, and 101.2 W, the $R_{\max}$ values are 61.4 μm, 63.5 μm, and 65.9 μm, and the maximum pressure points are located 26.9 μm, 23.3 μm, and 14.5 μm away from the collapsing bubble.

Table 1 provides the $R_{\max}/R_{\min}$ ratios, offering valuable insights into the volume change experienced by the bubble during collapse, serving as an indicator of its compression ratio. This ratio reflects the severity of the collapse (Kanthale *et al.*, 2008). For a 37 kHz ultrasonic frequency, $R_{\max}/R_{\min}$ ratios are 3.39, 6.71, and 10.41 at ultrasonic powers of 57.2 W, 83.6 W, and 132.3 W, respectively. Meanwhile, for an 80 kHz ultrasonic frequency, $R_{\max}/R_{\min}$ ratios are 3.63, 4.33, and 7.22 at ultrasonic powers of 46.3 W, 67.2 W, and 101.2 W, respectively. As the applied acoustic power increases, the bubbles experience higher negative pressure during the rarefaction cycle and higher positive pressure during the compression cycle, leading to an elevated compression ratio of the bubble cavity. This ratio increases alongside the collapsed interface velocity ($\dot{R}$), resulting in higher maximum pressures during the collapsed phase. Consequently, the force generated by the collapsing process increases. At an ultrasonic frequency of 37 kHz, this force is estimated to be 498.43 nN/μm^2, rising to 17 306.6 nN/μm^2 with increasing ultrasonic power. Similarly, at 80 kHz, the force increases from 633.04 nN/μm^2 to 5690.69 nN/μm^2 with increasing ultrasonic power.

4.2. Effect of energy and maximum pressure during collapse phase on the growth rate of microalgae

The total energy provided to the microalgae sample can be determined by taking into account the treatment period and ultrasonic power. The interaction between the total energy delivered to the microalgae and the relative specific growth rate of *B. braunii* microalgae during the two-day interval is shown in Fig. 2. *Botryococcus braunii* microalgae experienced an appropriate growth rate when ultrasonic energy was applied. The growth rate, however, changed from positive to negative when the microalgae received up to 30 kJ of total energy. In addition to specific growth rate, Table 2 shows biomass productivity.

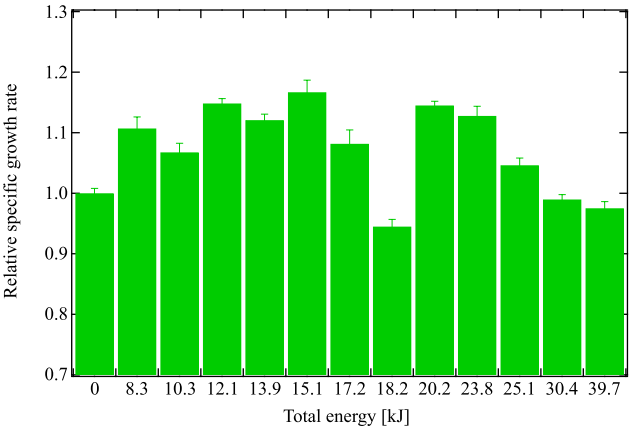

Fig. 2. Effect of total energy per excitation on the relative specific growth rate of *B. braunii* microalgae for a two-day interval. Error bars were used to represent the standard deviations derived from triplicate measurements of the data.

This shows that the number of microalgae cells decreased when subjected to a high level of energy from the ultrasonic wave compared to microalgae that were not exposed to ultrasonic energy. However, a negative growth rate is observed when the microalgae are exposed to an energy level of 18.2 kJ. Therefore, it is vital to consider other aspects of the ultrasonic wave.

Figure 3 displays the relationship between the maximum pressure generated during bubble collapse

Table 2. Specific growth rate of *B. braunii* under the influence of ultrasonic excitation from the logistic model and the biomass productivity.

Ultrasonic power [W]	Time/Energy [s/kJ]	Specific growth rate (r, day^{-1})	Biomass productivity (g $(L_{\text{day}})^{-1}$)
Frequency 37 kHz			
Control	0	0.282 ± 0.008	0.0361
57.2	180/10.3	0.301 ± 0.015	0.0421
83.6	180/15.1	0.329 ± 0.020	0.0486
132.3	180/23.8	0.318 ± 0.016	0.0435
57.8	300/17.2	0.305 ± 0.023	0.0403
83.6	300/25.1	0.295 ± 0.012	0.0454
132.3	300/39.7	0.275 ± 0.011	0.0287
Frequency 80 kHz			
Control	0	0.290 ± 0.007	0.0117
46.3	180/8.3	0.321 ± 0.019	0.0144
67.2	180/12.1	0.333 ± 0.008	0.0206
101.2	180/18.2	0.274 ± 0.012	0.0189
46.3	300/13.9	0.325 ± 0.010	0.0183
67.2	300/20.2	0.325 ± 0.007	0.0194
101.2	300/30.4	0.287 ± 0.008	0.0156

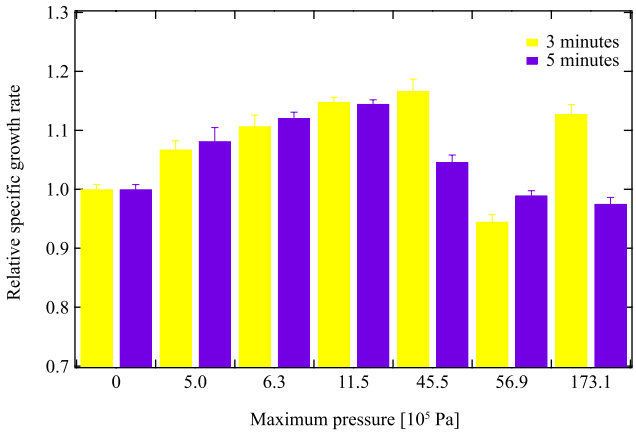

Fig. 3. Effect of maximum pressure during collapsing phase from $R_{\max}$ to $R_{\min}$ on the relative specific growth rate of *B. braunii* microalgae for a two-day interval. The yellow bar represents the exposure time of 3 min, and the purple color represents the exposure time of 5 min. Error bars were used to represent the standard deviations derived from triplicate measurements of the data.

and the relative specific growth rate of *B. braunii* microalgae. When the maximum pressure increases, up to a maximum pressure of 45.5 $\times 10^5$ Pa, the growth rate of *B. braunii* microalgae shows an increase. However, the specific growth rate of the microalgae becomes negative when the collapse pressure surpasses 56.9×10^5 Pa. This shows that the impact of the maximum pressure during bubble collapse has a negative impact on the growth of the *B. braunii* microalgae above this threshold.

In a previous scenario, exposing microalgae to ultrasonic energy of 18.2 kJ led to a decline in their growth rate. Examination of the maximum pressure during the collapse phase revealed potential contact between microalgae and collapsed cavity bubbles, reaching a maximum collapse pressure of 56.9×10^5 Pa. The force generated by the collapse was estimated based on this maximum pressure. Remarkably, the force exerted by the collapse of the bubble reached up to 5.7 $\mu N/\mu m^2$ when considering a typical spherical microalgal cell (*B. braunii*) with a diameter of approximately 9 µm (Tasić *et al.*, 2016). Consequently, the force applied to the microalgae was around 362.6 µN. In the report of Lee *et al.* (2012), the force required to rupture the cell wall of algae is about 11.33 µN, surpassing the threshold for growth inhibition in microalgae. In scenarios where maximum pressure exceeds 45.5 $\times 10^5$ Pa for the 3-minute exposure, the relative specific growth rate initially declines, followed by an increase. The study by Antony (1963) demonstrated that cavities occur at half-wavelength within the ultrasonic bath for each frequency. Therefore, ultrasonic frequencies of 37 kHz and 80 kHz have wavelengths of 40.41 mm and 18.69 mm, respectively. The distances between bubble collapse locations are approximately 20.21 mm and 9.35 mm for frequencies of 37 kHz and 80 kHz, respectively, with the latter being shorter than the former. Consequently, in the ultrasonic bath, the collapse positions for the 80 kHz ultrasonic wave exceeded those of the 37 kHz. This observation suggests that under the maximum pressure condition of 56.9×10^5 Pa, the microalgae were exposed to greater bubble collapse than in the 173.1×10^5 Pa maximum pressure condition, leading to inhibited specific growth rate.

The research findings demonstrate that the growth of *B. braunii* microalgae can be stimulated by various parameters. Among these conditions, the maximum

specific growth rate observed was 0.329 ± 0.020 day^{-1}, achieved when the microalgae cells were exposed to ultrasonic energy of 15.1 kJ and a maximum pressure during collapse of approximately 45.5×10^5 Pa. These conditions involved the application of 37 kHz ultrasonic frequency, with a three-minute exposure at a two-day interval. The stimulation of *B. braunii* microalgae by ultrasonic waves resulted in higher biomass productivity compared to microalgae not exposed to ultrasonic waves (Xu *et al.*, 2014). Moreover, cavitation phenomena generated by ultrasonic waves also contribute to nutrient and oxygen transport through membrane permeability, promoting the growth of *Echinacea purpurea*, *Staphylococcus epidermidis*, *Pseudomonas aeruginosa*, *Escherichia coli*, and *B. braunii* (Pitt, Ross, 2003; Xu *et al.*, 2014).

Ultrasound-induced cavitation in a medium involves the creation and oscillation of gas bubbles, which subsequently collapse near cells. This phenomenon converts potential energy into chemical, thermal, and mechanical energies in the form of reactive oxygen species (Topaz *et al.*, 2005). The interaction of cavitation near the cell involves a process known as sonoporation (Kudo *et al.*, 2009). Sonoporation refers to the transient and dynamic increase in cell membrane permeability, resulting from complex processes involving bubble physics and bubble-cell interactions (Fan *et al.*, 2014). When exposed to cavitation, microalgae cells with thin cell walls (e.g., *Chlamydomonas concordia*) or without cell walls (e.g., *Dunaliella salina*) are destroyed. However, cells with thick cell walls or those existing in colonies (e.g., *Nannochloropsis oculata*) tend to increase in population due to the ultrasound-induced separation of colonies, resulting in a higher number of individual cells or smaller colonies (Joyce *et al.*, 2014). It is possible that ultrasonic waves have caused fissures in the cell wall or separation of colonies, facilitating nutrient transport into the cells.

5. Conclusion

The study explored the impact of ultrasonic energy and maximum pressure during bubble collapse on the growth of *B. braunii* microalgae. Acoustic cavitation induced by ultrasonic waves generates cavitation bubbles that collapse explosively, creating pores near cell membranes and enhancing substrate conversion. Varied ultrasonic parameters, including frequency, power, exposure time, and intervals, were tested to stimulate microalgae growth. The influence of energy and the maximum pressure generated during bubble collapse was observed under all conditions when the exposure was extended to 2-day intervals. The reproduction of microalgae showed an enhancing trended until the energy exceeded 30 kJ. However, once the energy reached 18.2 kJ, the reproduction of microalgae was inhibited. This inhibitory effect can be attributed to the maximum pressure generated during the bubble bursting, which was found to reach 5.7 μN/μm^2 under these conditions. Considering a microalga with an approximate diameter of 9 μm, the resulting force is approximately 362.6 μN. Consequently, microalgae can restrain their reproduction when encountering bubble collapse events. The highest observed specific growth rate was 0.329 ± 0.020 day^{-1}, achieved with 15.1 kJ of ultrasonic energy, a maximum pressure of approximately 45.5×10^5 Pa, and 37 kHz ultrasonic frequency with a three-minute exposure at a two-day interval. This stimulation resulted in increased biomass productivity compared to untreated microalgae.

Acknowledgments

The author expresses gratitude for the financial support provided by the Royal Golden Jubilee (RGJ) Ph.D. Programme (grant no. PHD/0221/2560), through the National Research Council of Thailand (NRCT), and the Thailand Research Fund (TRF). The guidance of lecturers from the Division of Physics, Walailak University is also acknowledged.

References

1. Antony O.A. (1963), Technical aspects of ultrasonic cleaning, *Ultrasonics*, **1**(4): 194–198, doi: 10.1016/0041-624X(63)90167-7.

2. Brennen C. (2005), *Fundamentals of Multiphase Flow,* Cambridge University Press, pp. 345.

3. Chen J.T. *et al.* (2016), Preliminary assessment of Malaysian microalgae strains for the production of bio jet fuel, [in:] *IOP Conference Series Materials Science and Engineering*, **152**: 012042, doi: 10.1088/1757-899X/152/1/012042.

4. Dilia P., Kalsum L., Rusdianasari R. (2018), Fatty acids from microalgae *Botryococcus braunii* for raw material of biodiesel, *Journal of Physics: Conference Series*, **1095**: 012010, doi: 10.1088/1742-6596/1095/1/012010.

5. Enmak P. (2010), Influences of CO_2 concentrations and salinity on acceleration of microalgal oil as raw material for biodiesel production, *Journal of Biotechnology*, **150**: 19, doi: 10.1016/j.jbiotec.2010.08.063.

6. Fan Z., Kumon R.E., Deng C.X. (2014), Mechanisms of microbubble-facilitated sonoporation for drug and gene delivery, *Therapeutic Delivery*, **5**(4): 467–486, doi: 10.4155/tde.14.10.

7. Fu L., Li Q., Yan G., Zhou D., Crittenden J.C. (2019), Hormesis effects of phosphorus on the viability of *Chlorella regularis* cells under nitrogen limitation, *Biotechnology for Biofuels*, **12**: 121, doi: 10.1186/s13068-019-1458-z.

8. Gupte Y. (2012), Morpho-physiological characteristics of *Botryococcus braunii* (Kutzing, 1849) & its oil production from the species isolated from Thane, Maharashtra, India, *Asian Journal of Microbiology, Biotechnology and Environmental Sciences*, **14**(4): 523–526.

9. Hao X., Suo H., Peng H., Xu P., Gao X., Du S. (2021), Simulation and exploration of cavitation process during microalgae oil extracting with ultrasonic-assisted for hydrogen production, *International Journal of Hydrogen Energy,* **46**(3): 2890–2898, doi: 10.1016/j.ijhydene.2020.06.045.

10. Joyce E., King P., Mason T. (2014), The effect of ultrasound on the growth and viability of microalgae cells, *Environmental Biology of Fishes*, **26**: 1741–1748, doi: 10.1007/s10811-013-0202-5.

11. Kanthale P., Ashokkumar M., Grieser F. (2008), Sonoluminescence, sonochemistry (H_2O_2 yield) and bubble dynamics: Frequency and power effects, *Ultrasonics Sonochemistry*, **15**(2): 143–150, doi: 10.1016/j.ultsonch.2007.03.003.

12. Kudo N., Okada K., Yamamoto K. (2009), Sonoporation by single-shot pulsed ultrasound with microbubbles adjacent to cells, *Biophysical Journal*, **96**(12): 4866–4876, doi: 10.1016/j.bpj.2009.02.072.

13. Lee A.K., Lewis D.M., Ashman P.J. (2012), Disruption of microalgal cells for the extraction of lipids for biofuels: Processes and specific energy requirements, *Biomass and Bioenergy*, **46**: 89–101, doi: 10.1016/j.biombioe.2012.06.034.

14. Liu Y., Liu X., Cui Y., Yuan W. (2022), Ultrasound for microalgal cell disruption and product extraction: A review, *Ultrasonics Sonochemistry*, **87**: 106054, doi: 10.1016/j.ultsonch.2022.106054.

15. Onyeaka H., Miri T., Obileke K., Hart A., Anumudu C., Al-Sharify Z.T. (2021), Minimizing carbon footprint via microalgae as a biological capture, *Carbon Capture Science Technology*, **1**: 100007, doi: 10.1016/j.ccst.2021.100007.

16. Pereira R.N., Jaeschke D.P., Mercali G.D., Rech R., Marczak L.D.F. (2023), Impact of ultrasound and electric fields on microalgae growth: A comprehensive review, *Brazilian Journal of Chemical Engineering*, **40**: 607–622, doi: 10.1007/s43153-022-00281-z.

17. Pitt W.G., Ross S.A. (2003), Ultrasound increases the rate of bacterial cell growth, *Biotechnology Progress*, **19**(3): 1038–1044, doi: 10.1021/bp0340685.

18. Ren H.Y. *et al.* (2019), Ultrasonic enhanced simultaneous algal lipid production and nutrients removal from non-sterile domestic wastewater, *Energy Conversion and Management*, **180**: 680–688, doi: 10.1016/j.enconman.2018.11.028.

19. Rubsai A. (2012), *Isolation, growth characters and oil accumulation of green colonial microalgae, botryococcus braunii*, MS Degree, Walailak University.

20. Salaeh A., Boonphasuk S., Danworaphong S. (2017), Expediting growth rate of *Botryococcus braunii* using 37- and 80-kHz ultrasonic waves, [in:] *Proceedings of 24th International Congress on Sound and Vibration 2017* (*ICSV 24*), pp. 1782.

21. Shakirov Z.S., Khalilov I.M., Khujamshukurov N.A. (2021), Stress factors' effects on the induction of lipid synthesis of microalgae, *Journal of Applied Biology and Biotechnology*, **9**(06): 149–153, doi: 10.7324/JABB.2021.96019-1.

22. Tasić M.B., Pinto L.F.R., Klein B.C., Veljković V.B., Filho R.M. (2016), *Botryococcus braunii* for biodiesel production, *Renewable and Sustainable Energy Reviews*, **64**: 260–270, doi: 10.1016/j.rser.2016.06.009.

23. Topaz M. *et al.* (2005), Acoustic cavitation in phacoemulsification and the role of antioxidants, *Ultrasound in Medicine Biology*, **31**(8): 1123–1129, doi: 10.1016/j.ultrasmedbio.2005.02.016.

24. Wang M., Yuan W. (2016), Modeling bubble dynamics and radical kinetics in ultrasound induced microalgal cell disruption, *Ultrasonics Sonochemistry*, **28**: 7–14, doi: 10.1016/j.ultsonch.2015.06.025.

25. Wang S.K., Wang F., Stiles A.R., Guo C., Liu C.Z. (2014), *Botryococcus braunii* cells: Ultrasound-intensified outdoor cultivation integrated with in situ magnetic separation, *Bioresource Technology*, **167**: 376–382, doi: 10.1016/j.biortech.2014.06.028.

26. Xu L., Wang S., Wang, F., Guo C., Liu C.Z. (2014), Improved biomass and hydrocarbon productivity of *Botryococcus braunii* by periodic ultrasound stimulation, *BioEnergy Research*, **7**: 986–992, doi: 10.1007/s12155-014-9441-9.

27. Zhang L., Li B., Wu Z., Gu L., Yang Z. (2016), Changes in growth and photosynthesis of *Mixotrophic Ochromonas sp.* in response to different concentrations of glucose, *Journal of Applied Phycology*, **28**: 2671–2678, doi: 10.1007/s10811-016-0832-5.